Angewandte Chemie
Eine Zeitschrift der Gesellschaft Deutscher Chemiker

Supporting Information

ATP-Mediated Transient Behavior of Stomatocyte Nanosystems

Hailong Che, Jianzhi Zhu, Shidong Song, Alexander F. Mason, Shoupeng Cao, Imke A. B. Pijpers, Loai K. E. A. Abdelmohsen, and Jan C. M. van Hest**

anie_201906331_sm_miscellaneous_information.pdf
anie_201906331_sm_Video_S1.avi
anie_201906331_sm_Video_S2.avi
anie_201906331_sm_Video_S3.avi

Table of content:

1) **Materials**
2) **Instruments**
3) **Synthesis**
4) **Stomatocyte assembly**
5) **Methods and analysis**
6) **References**

Materials

Poly(ethylene glycol) methyl ether and poly(ethylene glycol) (M_n 2 kg/mol, Sigma, 99%), α-bromoisobutyryl bromide (Sigma, 99%), trimethylamine (Sigma, 98%), styrene (Sigma-Aldrich, 98%) N,N,N',N",N"-pentamethyl-diethylenetriamine (PMDETA) (Sigma, 99%), dibenzocyclooctyne-amine (Sigma), N^{ε}-carbobenzyloxy-L-lysine N-carboxy anhydride (LysZ NCAs, Sigma) K_2PtCl_4 (Alfa Aesar, 98%), ascorbic acid (TCI), poly(vinyl pyrrolidone) (PVP, M_W= 10,000, Sigma), 3,3'-dimethoxybenzidine (DMB, Sigma, 98%), horseradish peroxidase (HRP, Sigma) were used as received. Copper (I) bromide (CuBr, Sigma, 99.99%) was purified by stirring in acetic acid, followed by washing with acetone three times. N_3-PEG2K-OH was synthesized according to a literature procedure.[1]

Instruments

Nuclear Magnetic Resonance Spectroscopy (NMR). ^{1}H NMR spectra were recorded on a Bruker (400MHz) spectrometer with $CDCl_3$, DMSO and D_2O as the solvents and TMS as an internal standard.

Gel permeation chromatography (GPC). The molecular weights and dispersities of the polymers were characterized by GPC. GPC measurements were conducted using a Shimadzu Prominence-i SEC system with a PL gel 5 µm mixed D and mixed C column (Polymer Laboratories) with PS standard and equipped with a Shimadzu RID-20A differential refractive index detector. THF was used as an eluent with a flow rate of 1 mL min^{-1}.

Dynamic Light Scattering (DLS) and Zeta Potential (ζ). A Malvern Z90 Zetasizer equipped with a 633 nm He−Ne laser and an avalanche photodiode detector was used to characterize the hydrodynamic size and surface zeta potential of the particles. The scattering light at a 90° angle was detected and used to analyze the size and distribution.

Transmission Electron Microscopy (TEM). TEM images were recorded by a FEI Tecnai 20 (type Sphera) at 200 kV. 10 µL of a sample was dropped onto a carbon-coated copper grid. After removing the excess solution by blotting paper, the samples were dried at ambient conditions.

Cryogenic transmission electron microscopy (cryo-TEM). Experiments were performed using a FEI Tecnai G2 Sphera (200 kV electron source) equipped with LaB6 filament utilizing a cryoholder or a FEI Titan (300 kV electron source) equipped with autoloader station. Samples for cryo-TEM were prepared by treating the grids (Lacey carbon coated, R2/2, Cu, 200 mesh, EM sciences) in a Cressington 208 carbon coater for 40 seconds. Then, 3 µl of the polymersome solution was pipetted on the grid and blotted in a Vitrobot MARK III at 100% humidity. The grid was blotted for 3 seconds (offset -3) and directly plunged and frozen in liquid ethane.

Scanning electron microscopy (SEM). SEM images were obtained on a JEOL 6330 Scanning Electron Microscope. To prepare SEM samples, 10 µL of the sample was dropped onto a small piece of silicon wafer, and the samples were dried at room temperature.

Nanosight. To track the movement of the particles, a Nanosight LM10HS instrument (Malvern Instruments) equipped with an Electron Multiplication Charge Coupled Device (EMCCD) camera was used. The camera was mounted on an optical microscope in order to track the light scattered by the injected particles that are present in the focus of an 80 µm beam generated by a single mode laser diode with a 60 mW blue laser (405 nm). The concentration of the particles was between 10^7 and 10^9 particles mL^{-1}. Samples were injected into the nanosight chamber which has a 0.5 mL volume. The mean square displacement (MSD) of the particles was extracted from NTA 2.2 software.

Asymmetric Flow Field-Flow Fractionation. The asymmetric flow field-flow fractionation-UV-Quels (AF4-UV-Quels) experiments were performed on a Wyatt Dualtec AF4 instrument connected to a Shimadzu LC-2030 Prominence-i system with a Shimadzu LC-2030 autosampler. The AF4 was connected to a Wyatt DAWN HELEOS II light scattering detector (MALS) installed at different angles (12.9 º, 20.6 º, 29.6 º, 37.4 º, 44.8 º, 53.0 º, 61.1 º, 70.1 º, 80.1 º, 90.0 º, 99.9 º, 109.9 º, 120.1 º, 130.5 º, 149.1 º, and 157.8 º) using a laser operating at 664.5 nm and a Wyatt Optilab Rex refractive index detector. Detectors were normalized using Bovine Serum Albumin (BSA). The processing and analysis of the LS data and radius of gyration (R_g) calculations were performed on Astra 7 software (using the Berry model, which is recommended for particles of size > 50 nm). All AF4 fractionations were performed on an AF4 short channel with regenerated cellulose (RC) 10 kDa membrane (Millipore) and a spacer of 350 µm.

Ultraviolet–visible Spectroscopy (UV/Vis). The UV absorbance spectra were recorded on a Jasco V-650 UV/Vis spectrometer at 293 K.

Synthesis

Synthesis of $mPEG_{45}$-*b*-PS_{210} and N_3-PEG_{45}-*b*-PS_{215}

The reaction scheme to PEG-*b*-PS was as follows (Supplementary Scheme 1):

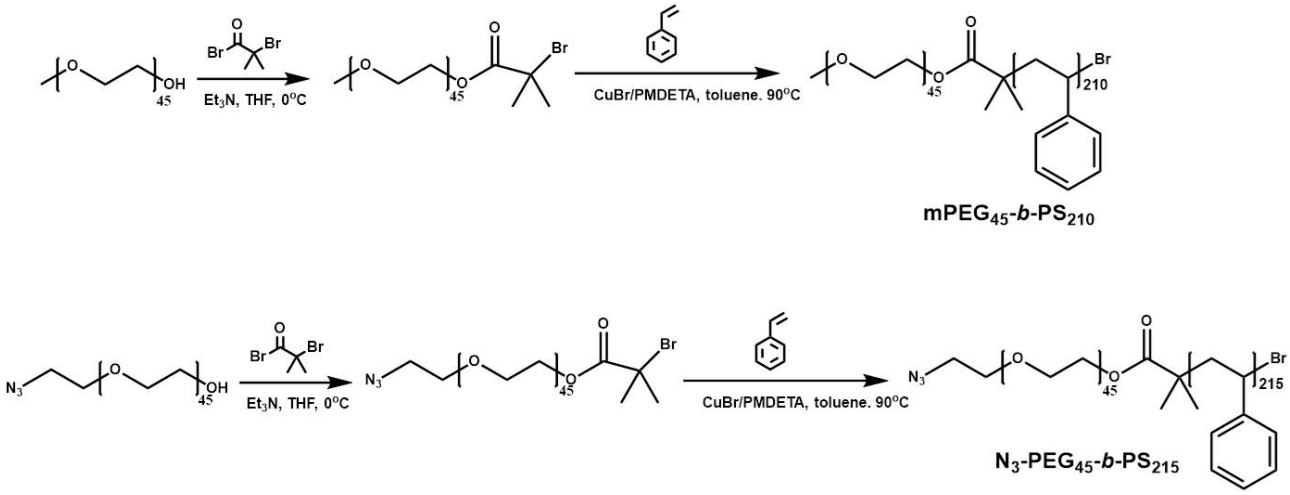

Scheme S1. Synthetic route of $mPEG_{45}$-*b*-PS_{210} and N_3-PEG_{45}-*b*-PS_{215}.

ATRP macro-initiator $mPEG_{45}$-Br and N_3-PEG_{45}-Br were prepared according to literature.[2] $mPEG_{45}$-*b*-PS and N_3-PEG_{45}-*b*-PS were synthesized by atom transfer radical polymerization (ATRP). Briefly, $mPEG_{45}$-Br or N_3-PEG_{45}-Br (100 mg, 0.05 mmol), styrene(2.6 g, 25 mmol) and CuBr (7 mg, 0.05 mmol) were added into a 5 mL round bottom flask, followed by degassing with nitrogen for 30 min. Subsequently, PMDETA (10 μL, 0.05 mmol) dissolved in 0.5 mL toluene was added to the flask, after which the mixture was purged with nitrogen for another 30 min. Then the flask was placed into a 90 °C oil bath. After the desired monomer conversion was reached, the solution was immersed in a liquid nitrogen bath in order to stop the radical polymerization. Then the solution was diluted in 50 mL of THF and passed through a neutral alumina column twice to remove the copper catalyst. Then the filtrate was concentrated and precipitated into 50 mL methanol twice. The white precipitate was collected and dried in a vacuum oven at room temperature for 24 h. With ^{1}H NMR (Figure S1), the PS polymerization degrees (DPs) of $mPEG_{45}$-*b*-PS and N_3-PEG_{45}-*b*-PS were determined, which are 210 and 215, respectively. The molecular weight and molecular weight distribution were determined by GPC using THF as the eluent (Figure S2).

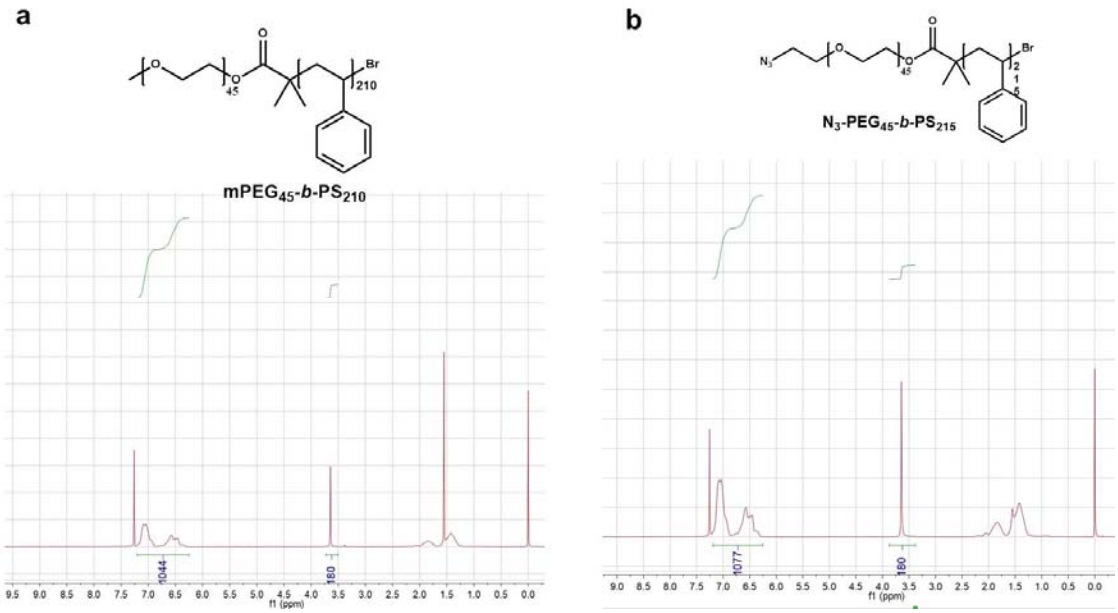

Figure S1. ^{1}H-NMR spectra of (a) mPEG$_{45}$-*b*-PS$_{210}$ and (b) N$_3$-PEG$_{45}$-*b*- PS$_{215}$ in CDCl$_3$.

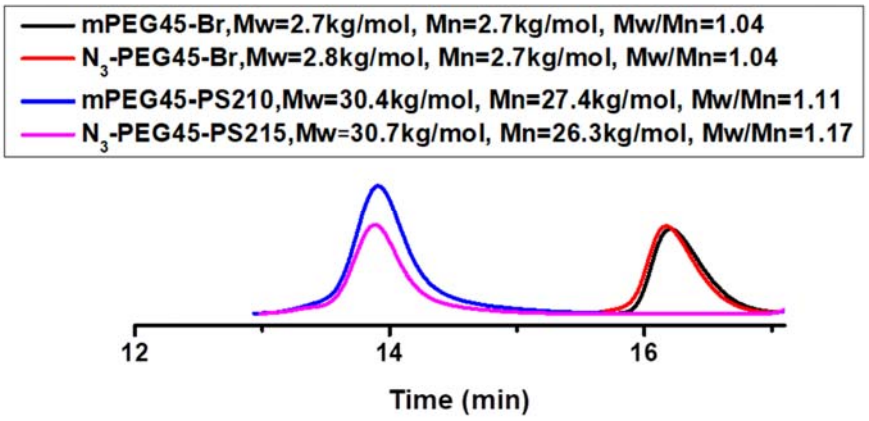

Figure S2. GPC traces of mPEG$_{45}$-Br (black), N$_3$-PEG$_{45}$-Br (red), mPEG$_{45}$-*b*-PS$_{210}$ (blue) and N$_3$-PEG$_{45}$-*b*-PS$_{215}$ (purple), respectively.

Synthesis of DBCO- poly-L-lysine (DBCO-PLL)

The reaction scheme to DBCO-PLL was as follows (Supplementary Scheme 2):

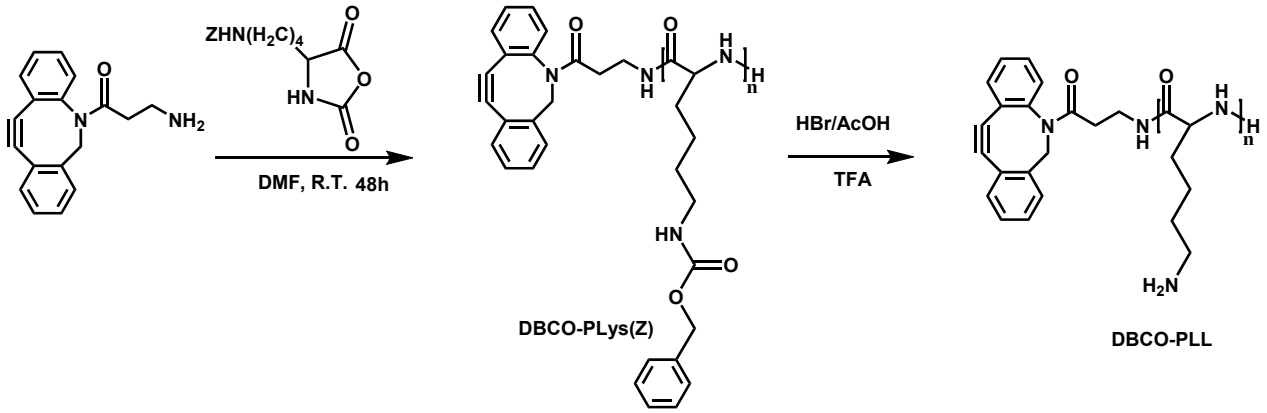

Scheme S2. Synthetic route toward DBCO-PLL.

Synthesis of DBCO-poly(N$^{\varepsilon}$-carbobenzyloxy-L-lysine) (DBCO-PLZ)

The synthesis was modified from previous literature reports.[3] LysZ NCA (3 g, 10 mmol) and DBCO-NH_2 (13.8 mg, 0.05 mmol) were dissolved in 20 mL anhydrous *N,N*-dimethylformamide (DMF). Then the mixture was allowed to react at room temperature for 48 h under nitrogen. ^{1}H NMR (400 MHz, DMSO-d6, ppm): 8.02 (w, -NH), 7.4-7.17 (s, C_6H_5 in Z), 5.0 (s, CH_2 in Z group), 2.8 and 1.80-1.15 (m,-CH_2 in pLys).The ^{1}H NMR result before purification confirmed that all the monomers were converted into polymer, suggesting that the DP of PLZ is 200 (Figure S3a). After most of the solvent was removed by evaporation, the mixture was precipitated in excess cold diethyl ether. The precipitates were purified by repeated filtration and then dried in a vacuum oven at room temperature for 24 h.

Synthesis of DBCO-poly(L-lysine) (DBCO-PLL)

DBCO-PLZ_{200} (600 mg, 0.01 mmol) dissolved in 10 mL DMF with 10% trifluoroacetic acid was added to a 33% solution of HBr in acetic acid (0.55 g, 0.35 mmol). The reaction was performed for 3 h at room temperature, and then precipitated in excess cold diethyl ether. The solid was washed several times with diethyl ether and dried under vacuum. The obtained dry solid was dissolved in distilled water, transferred into a dialysis bag (molecular weight cutoff: 12,000-

14,000 Da, flat width 25 mm) and dialyzed against water. Finally the product was obtained by freeze-drying. ^{1}H NMR (400 MHz, D_2O, ppm): 8.2-7.9 (w, -NH), 4.25 (w, -CH), 2.8 and 1.64-1.21 (m, -CH_2 in pLys). The resonances of the phenyl protons (-C_6H_5, 7.4-7.17 ppm) and methylene protons (-CH_2, 5.0 ppm) of the Z groups in PLZ disappeared, confirming the successful deprotection of ε-amine of the lysine side chains (Figure S3b).

Control polymer DBCO-PLL_{100} was synthesized according to the procedure similar to that of DBCO-PLL_{200}. Unless stated otherwise, PLL-stomatocytes indicate PLL_{200} modified stomatocytes.

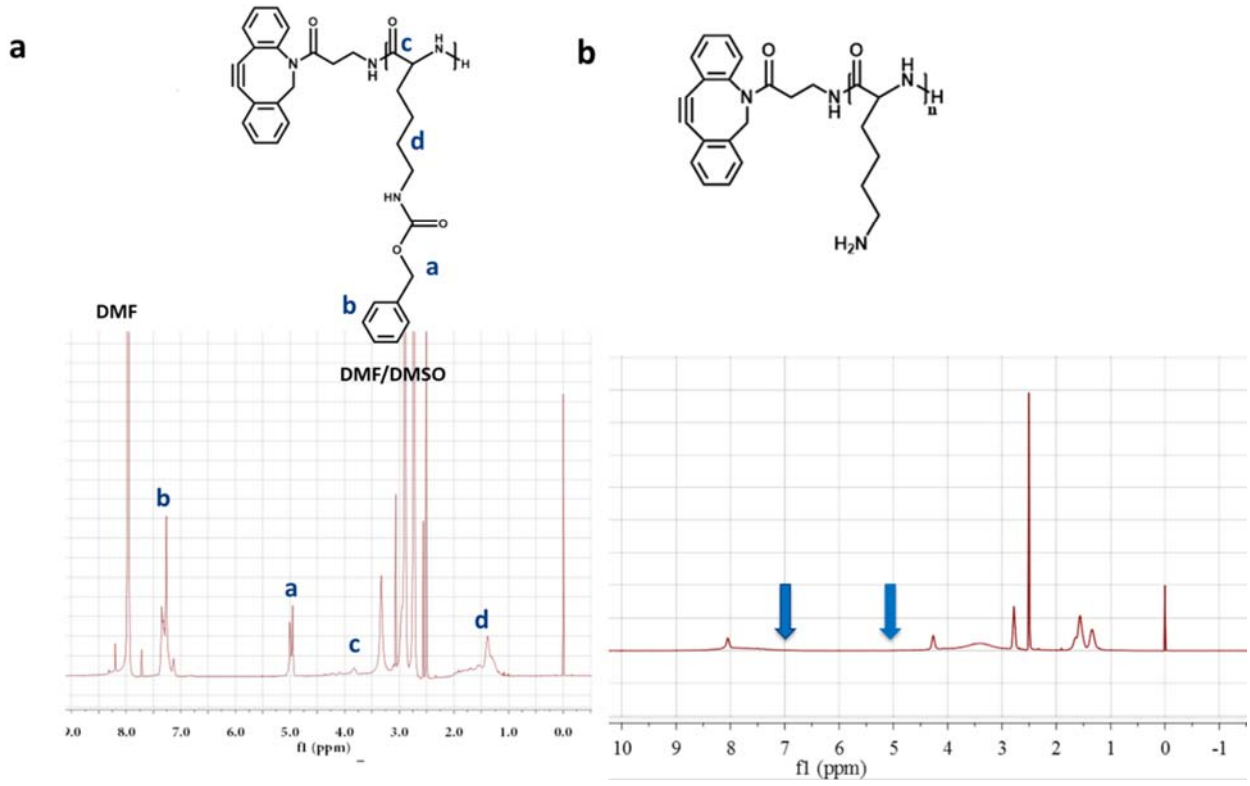

Figure S3. ^{1}H-NMR spectra of (a) unpurified DBCO-PLZ_{200} in DMSO-d_6 and (b) DBCO-PLL_{200} in D_2O.

Stomatocyte assembly

Preparation of stomatocytes with encapsulated HRP

$mPEG_{45}$–*b*-PS_{210} (9 mg) and N_3-PEG_{45}-*b*-PS_{215}(1 mg) were dissolved in a 1 mL mixture of THF/dioxane (80:20 v/v), followed by addition of 0.6 mL Milli-Q water *via* a syringe pump at a rate of 1 mL h^{-1}. Then 0.4 mL Milli-Q water containing 1 mg HRP was added at the same rate. Next, the resulting cloudy polymersome/HRP mixture was transferred into a dialysis bag(molecular weight cutoff: 12,000-14,000 Da, flat width 25 mm) and dialyzed against 50 mM sodium chloride with the dialysis solution changed after one hour to generate almost “closed” stomatocytes. After 24 h, the stomatocyte and enzyme mixture was centrifuged for 5 min at 5000 rpm *via* spin filtration over 0.22 μm membranes. The filtrate was withdrawn and fresh medium was added. This centrifugation process was repeated until no obvious absorption at 403 nm (HRP’s characteristic Soret band) was observed from the filtrate, which indicates that free enzymes were completely removed from the stomatocyte solution.

Preparation of PtNPs loaded stomatocytes

$mPEG_{45}$–*b*-PS_{210} (9 mg) and N_3-PEG_{45}-*b*-PS_{215} (1 mg) were dissolved in a 1 mL mixture of THF/dioxane (80:20 v/v), followed by addition of 1 mL Milli-Q water via a syringe pump at a rate of 1 mL h^{-1}. Then the resulting cloudy polymersome solution was transferred into a dialysis bag (molecular weight cutoff: 12,000-14,000 Da, flat width 25 mm) and dialyzed against 50 mM sodium chloride with the dialysis solution changed after one hour to generate almost “closed” stomatocytes. After 24 h, the stomatocyte solution was concentrated to 1 mL with a final polymer concentration of 10 mg mL^{-1}. Then PtNPs were in situ formed inside the stomatocytes. More specifically, 8.8 mg ascorbic acid was completely dissolved in 0.5 mL Milli-Q water, after which 0.5 mL of a 20 mM aqueous solution of K_2PtCl_4 and 5 mg PVP was added. Then, 0.5 mL of the above mentioned stomatocyte solution was added. The mixture was allowed to stir for 30 min, followed by sonication at room temperature for one hour. Free PtNPs were removed via spin filtration over 0.22 μm membranes. The PtNPs loading efficiency is around 35 % (35% of the cavities contain nanoparticles) according to TEM images of 100 stomatocytes.

Preparation of PLL-modified HRP or PtNPs loaded stomatocytes

To decorate the surface of the stomatocytes with PLL, 1.5 mg DBCO-PLL_{100} or 3 mg DBCO-PLL_{200} was added to the above prepared HRP or PtNP loaded stomatocytes. Then the mixture was stirred for 24h at room temperature. Subsequently, free polymers were removed *via* spin filtration over 0.22 μm membranes (Supplementary Scheme 3 and Scheme 4). The purified stomatocyte solution was lyophilized, and the weight change of the sample was utilized to calculate the coupling efficiency, which is around 94 %.

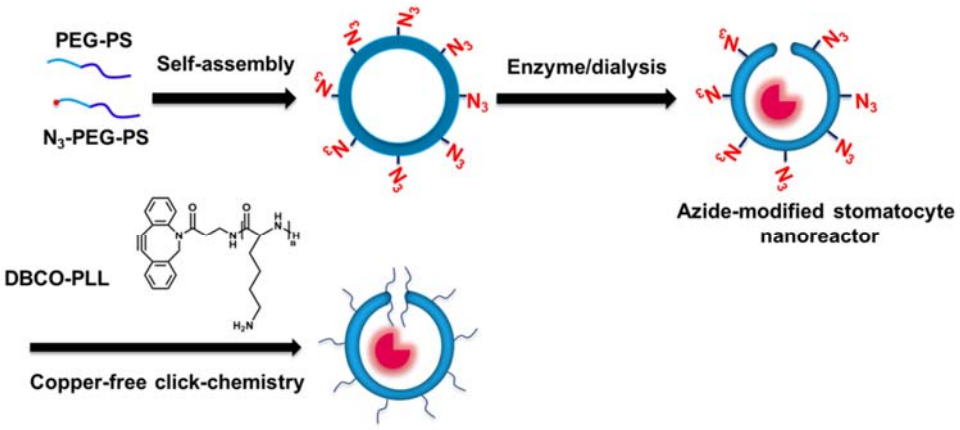

Scheme S3. Formation of PLL-modified stomatocyte nanoreactors.

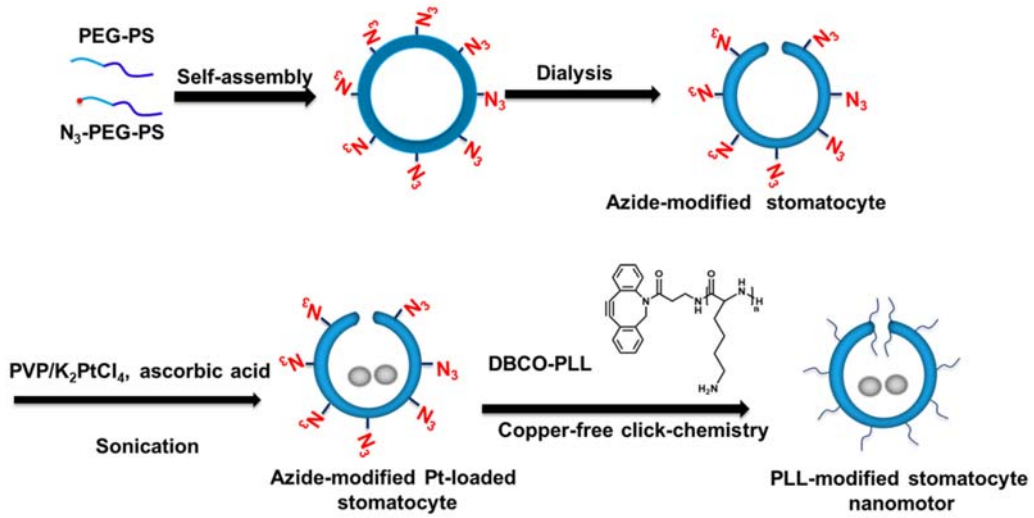

Scheme S4. Formation of PLL-modified stomatocyte nanomotors.

Methods and analysis

Morphology characterization of the stomatocytes

The morphology of the prepared stomatocytes was investigated by TEM and Cryo-TEM. The introduction of PLL on the surface of the stomatocytes did not have any influence on the final structure of the stomatocytes (Figure S4 and S5).

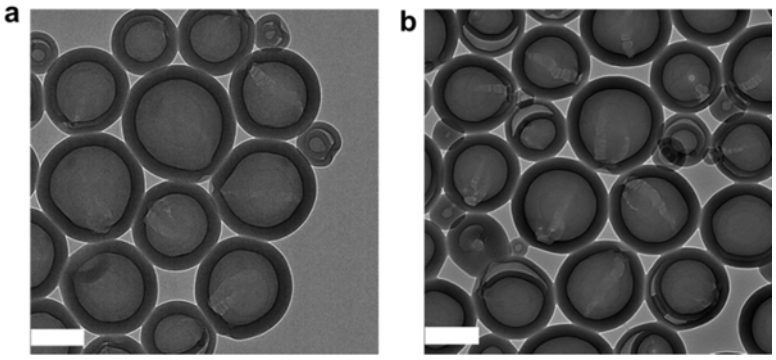

Figure S4. TEM images of (a) stomatocytes and (b) PLL-modified stomatocytes after six months storage at room temperature. All scale bars are 200 nm.

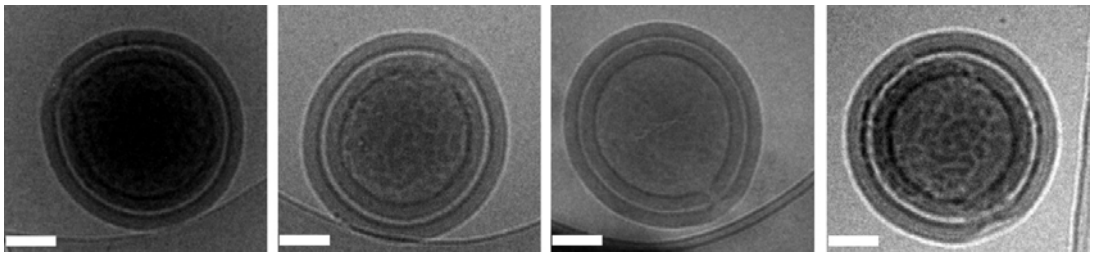

Figure S5. Cryo-TEM images of the PLL-stomatocytes. All scale bars are 100 nm.

Size distributions of the nanoparticles

The sizes and size distributions of stomatocytes, PLL-stomatocytes, HRP-loaded PLL-stomatocytes, and Pt-loaded PLL-stomatocytes were measured with a Malvern DLS-Zetasizer (Table S1). The attachment of PLL on the surface of the stomatocytes did not induce a size change of the particles as only 10% of the block copolymers was modified by PLL. The encapsulation of PtNPs gave rise to an approximate 20 nm size increase compared with empty stomatocytes and HRP loaded stomatocytes, which might be caused by the entrapment of PtNPs.

Table S1 DLS results of empty stomatocytes, HRP loaded stomatocytes, HRP loaded PLL-stomatocytes, PtNPs, PtNP loaded stomatocytes, and PtNPs loaded PLL-stomatocytes, respectively.

Sample	Size (nm)	PDI
Stomatocytes	375	0.096±0.02
HRP loaded stomatocytes	380	0.102±0.02
HRP loaded PLL-stomatocytes	378	0.105±0.03
PtNPs	45	0.103±0.02
PtNPs loaded stomatocytes	395	0.098±0.03
PtNPs loaded PLL-stomatocytes	393	0.116±0.02

Zeta potential of the nanoparticles

The surface charge changes of the stomatocytes, N_3-stomatocytes, and PLL-stomatocytes were measured by a Malvern DLS-Zetasizer. The ATP effects on the zeta potential of the nanoparticles were performed as follows: ATP in different concentrations was added to the PLL-stomatocyte solution, and the zeta potential of the mixtures was measured after 60 s. To show that only PLL could interact with ATP to form complexes, the zeta potential changes of the stomatocytes and N_3-stomatocytes without PLL after addition of ATP were studied (Figure S6). Also, the AMP effect on the surface charge change of the nanoparticles compared with ATP was investigated. To study the dynamic zeta potential change of the nanoparticles induced by apyrase, the PLL-stomatocytes were first complexed with ATP (the charge ratio r=1), after which apyrase was applied at different concentrations. The zeta potential changes were recorded every two minutes.

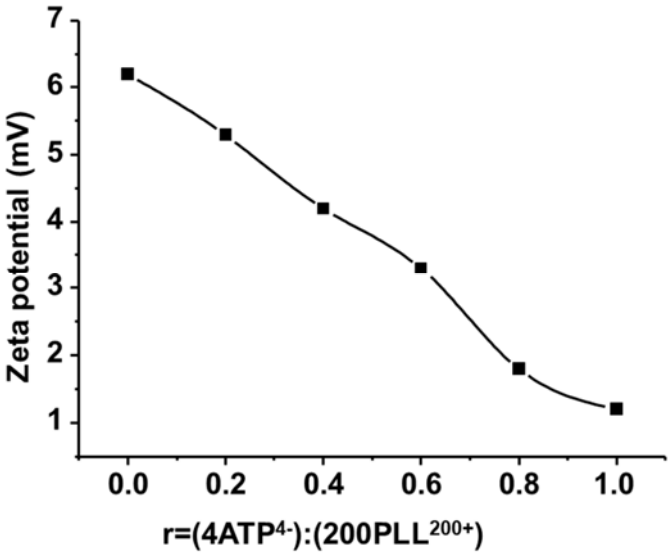

Figure S6. The zeta potential change of the PLL-stomatocytes in the presence of ATP at different concentrations.

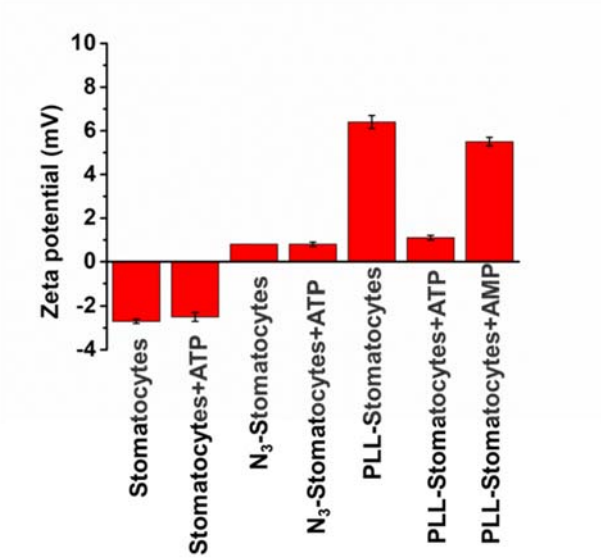

Figure S7. ATP effect on the zeta potential of the stomatocytes, azide- stomatocytes, and PLL-stomatocytes, respectively. These results show that the surface charge change of the stomatocytes was caused by ATP/PLL binding. ATP does not have interactions with stomatocytes or N_3-stomatocytes, and the interaction between AMP and PLL is negligible. Experimental conditions: 0.5 mg mL^{-1} nanoparticles in MES buffer (5 mM, pH 6.5) and 62.5 μM ATP or 125 μM AMP.

Enzyme encapsulation efficiency

The complete removal of HRP was confirmed by size exclusion chromatography (SEC) (Figure S8). Encapsulated HRP was released from the stomatocytes by reshaping the bowl-shaped structures back into polymersomes by addition of 200 µL of THF/dioxane (4:1, v/v) directly to the nanoreactors (Figure S9). The released enzymes were collected for analysis of the incorporation efficiency, which was calculated as 9.5% by bicinchoninic acid (BCA) assay. A BCA Protein Assay Kit was purchased from ThermoFisher. The enzyme concentration was determined using a standard BCA protein assay protocol. Briefly, a standard curve of the enzyme was first established using the native enzyme with a series of enzyme concentrations (10 mg mL^{-1}, 8 mg mL^{-1}, 6 mg mL^{-1}, 4 mg mL^{-1}, 2 mg mL^{-1} and 1 mg mL^{-1}). 25 µL of each standard or unknown sample was pipetted into a microplate well, then 200 µL of the BCA working reagent (50:1, Reagent A:B) was added to each well and the solution was mixed thoroughly on a plate shaker for 30 seconds. After incubation at 37°C for 30 min, the absorbance at 562 nm was recorded in the plate reader. The enzyme concentration was calculated referring to the standard curve.

Confirmation of successful encapsulation of enzymes and PtNPs inside the stomatocytes

To confirm that the enzymes were successfully encapsulated inside the stomatocytes, the AF4 technique was applied. Aliquots of free HRP, empty stomatocytes and HRP-encapsulated stomatocytes were injected in the AFFF separation channel. Enzymes were first eluted while the stomatocytes or HRP loaded stomatocytes were eluted much later owing to their smaller diffusion coefficient. A general method for the AF4 elution of the stomatocytes is shown in Table S2. The same analysis method was used to characterize the encapsulation of PtNPs inside the stomatocytes.

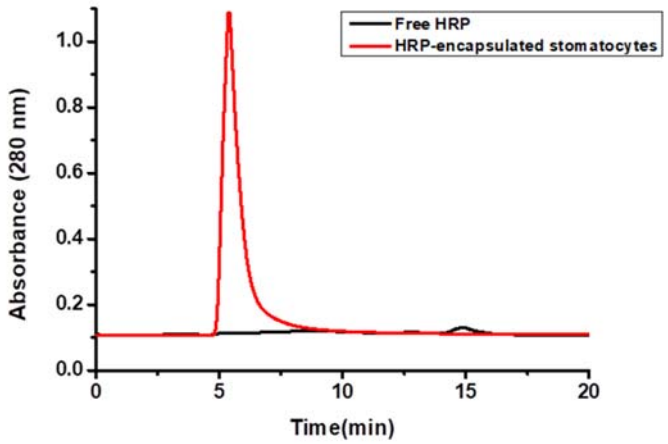

Figure S8. Normalized preparative SEC traces of HRP-loaded stomatocytes (red trace) and that of the free HRP enzyme (black trace) in MES buffer (5 mM, pH 6.5). In each case, the injection volume was 1 mL, and the absorbance of the enzyme was 280 nm.

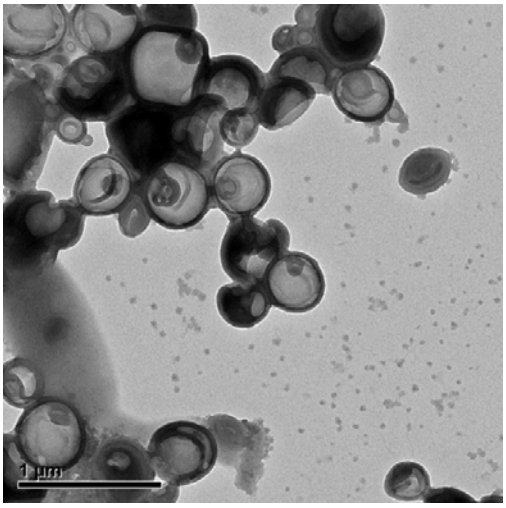

Figure S9. TEM image of the polymersomes reshaped by addition of organic solvent to the stomatocyte solution.

Determination of HRP activities

The activity of HRP-loaded stomatocytes was determined by means of activity assays for HRP using DMB as a substrate. The formation of the oxidized products was monitored by UV−vis spectroscopy. The activity assay was performed at room temperature in 1 cm silica glass cuvettes by mixing 0.8 mL MES buffer solution (5 mM, pH 6.5) of the HRP-encapsulated stomatocytes (0.1 mg mL^{-1}) and DMB. The enzymatic reaction was started by the addition of 10 µL H_2O_2 solution. The final concentrations for HRP, DMB and H_2O_2 were 5 U mL^{-1}, 400 µM and 100 mM, respectively. Absorbance at 492 nm was recorded every 60 s. As a control experiment, a free HRP activity assay with DMB as substrate was carried out at the same experimental conditions (Figure S10). The relative activity of the nanoreactors was calculated by comparing the different slopes of the absorption increase in the original linear phase condition.

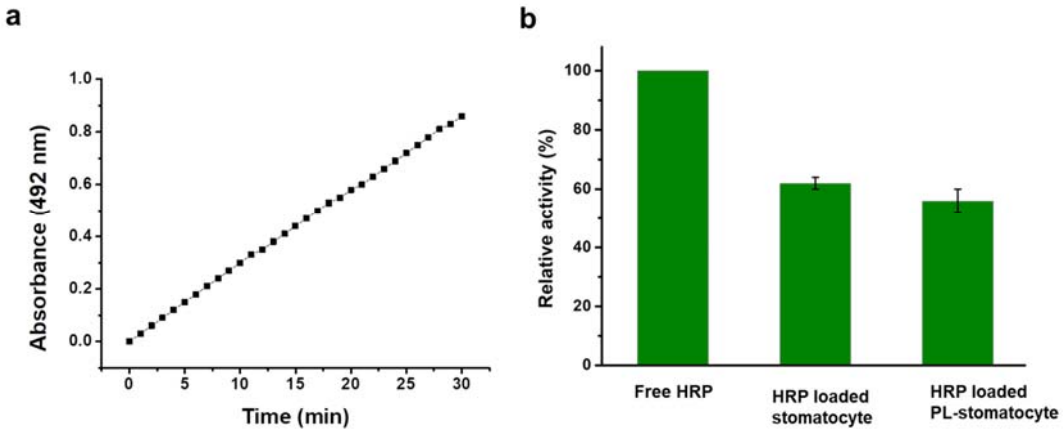

Figure S10. Activity assay of (a) free HRP and (b) HRP loaded stomatocyte nanoreactors with DMB as substrate at pH 6.5 (HRP: 5 U mL^{-1}; DMB: 400 µM; H_2O_2: 100 mM).

Table S2. General method for the AF4 fractionation of the stomatocytes. The flow conditions applied were as follows: 0.7 mL min^{-1} detector flow, 1.50 mL min^{-1} focus flow and 0.20 mL min^{-1} injection flow.

Start time (min)	End time(min)	Mode	Cross flow start (mL min^{-1})	Cross flow end (mL min^{-1})
0	2	Elution	1.00	1.00
2	3	Focus	-	-
3	6	Focus + inject	-	-
6	8	Elution	1.00	1.00
8	9	Elution	1.00	0.50
9	21	Elution	0.50	0.50
21	23	Elution	0.50	0.00
23	35	Elution	0.00	0.00
35	36	Elution	0.00	0.00
36	37	Elution + inject	0.00	0.00
37	40	Elution	0.00	0.00

ATP-mediated nanoreactors

10 μL ATP was added in 0.75 mL MES buffer solution (5 mM, pH 6.5) containing the HRP-encapsulated PLL-stomatocytes (0.5 mg mL^{-1}). Then 10 μL H_2O_2 and 10 μL DMB were added. Absorbance at 492 nm was recorded every 60 s. ATP at different concentrations (25 μM, 50 μM and 62.5 μM) was added to study the ATP-controlled biocatalytic reaction. To reopen the nanoreactors, 62.5 μM ATP with the charge ratio r=1, where r=($4ATP^{4-}$:($200PLL^{200+}$) was first added, after which 5 μL apyrase was introduced to hydrolyze ATP. The influence of different apyrase concentrations (0.05 U mL^{-1}, 0.1 U mL^{-1} and 0.15 U mL^{-1}) on the reactivation of the nanoreactors was studied. To study the effect of apyrase on the enzymatic reaction of the nanoreactors, ATP was introduced before adding apyrase. Please note that the enzymatic reaction is almost constant at the last stages (ca. 40 - 60 min), which may be ascribed to the accumulation of products.

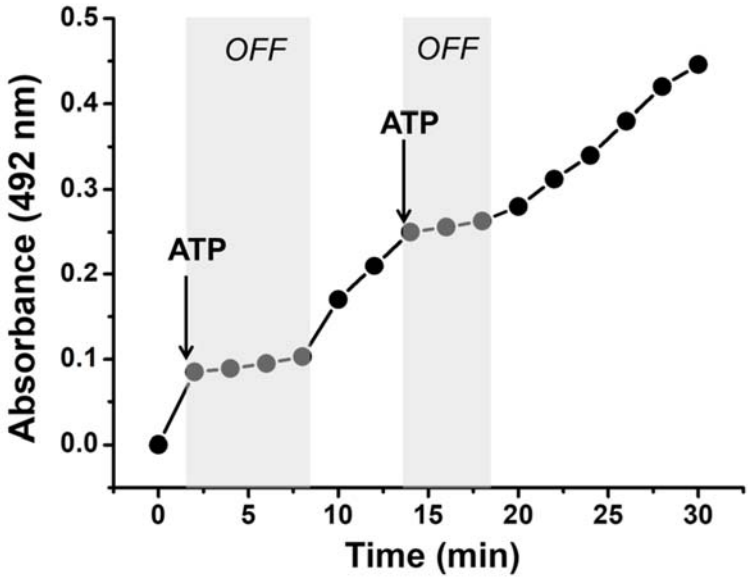

Figure S11. UV absorbance at 492 nm of the oxidation of DMB by PLL-stomatocyte nanoreactors upon the repeated addition of ATP in the presence of 0.15 U/mL apyrase. Experimental conditions at the two points of addition: ATP: 62.5 μM, 0.5 mg mL^{-1} PLL-stomatocytes; MES buffer (5 mM, pH 6.5) and [DMB]=400 μM.

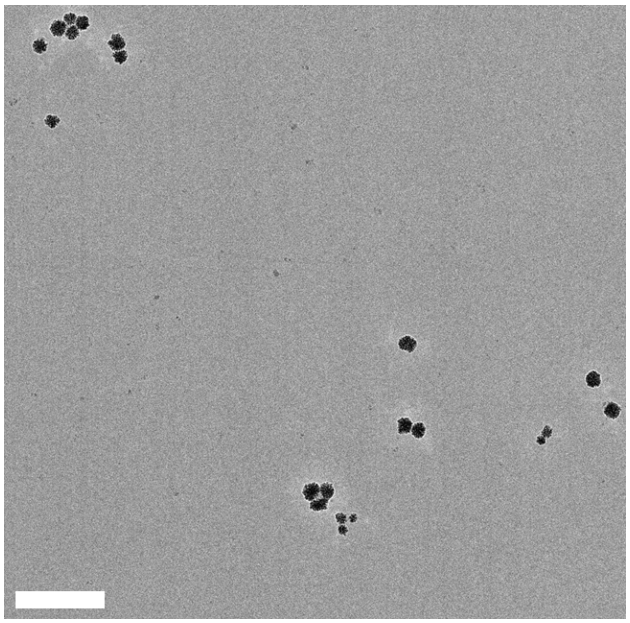

Figure S12. TEM image of PtNPs. Scale bar is 200 nm.

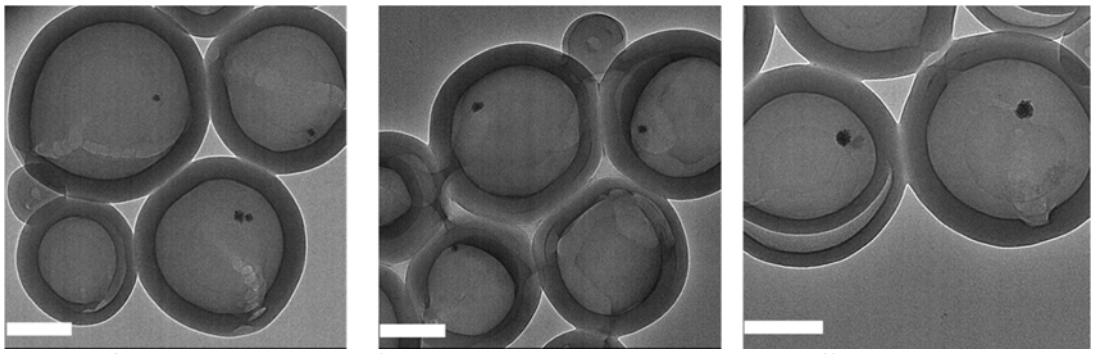

Figure S13. TEM images of PtNP loaded stomatocytes at different grid areas. All scales bars are 100 nm.

Movement analysis

To study in detail the transient behavior of the nanoparticles nanoparticle-tracking analysis (NTA) was used to follow, in real time, the motion of the stomatocytes and calculate their average mean square displacement (MSD). Such a technique was previously implemented to analyze the speed of stomatocytes nanomotors.[4] The NTA technique allows bi-dimensional extraction of coordinates (*x, y*) by measuring the trajectories of single particles. Per each experiment, 20 stomatocyte nanoparticles were tracked for 30 s. In order to analyze the motion of our platinum-encapsulated stomatocytes it was recorded at different concentrations of H_2O_2. According to Golestanian's self-diffusiophoretic model,[5] we could calculate the average velocity or speed of the motors based on MSD curves. According to this model, the motion of particles in medium with low Reynolds number is a net result of the contribution of rotational and translational velocity. This diffusiophoretic model suggests that a linear component of the mean squared displacement (MSD) curves according to equation $\Delta r^2 = (4D)\Delta t$ can be extracted if the observed particles are in Brownian motion. Indeed, this was the case when there was no H_2O_2 added to the system (Figure S14, Supporting Information). In another control experiment whereby H_2O_2 was added to empty stomatocytes confirmed that hydrogen peroxide did not affect neither the Brownian motion nor the extracted trajectories, and a linear MSD fitting was extracted (Figure S15, Supporting Information). Addition of H_2O_2 (at different concentrations) to platinum-loaded stomatocytes resulted in a (propulsive) directional motion. The rotational velocity coefficient along the symmetry axis of our stomatocytes (which has an average radius of 250 nm) is described by the equation $D_r = \tau_r^{-1} = TK_B/(8\pi\eta R^3)$, where τ_r is reorientation time. At 25 °C (the average temperature of the experiments) the reorientation time of the stomatocytes is 0.095 s, which is relatively rapid. Such a rapid τ_r would cause such stomatocytes to undergo a random walk for long Δt and translational velocity can be observed for short Δt. According to the self-diffusiophoretic model, the equation $\Delta r^2 = (4D)\Delta t + (v^2)(\Delta t^2)$ was used to extract the MSD of moving particles and when Δt is smaller than τ_r, the MSD would display a non-linear fitting. In presence of high H_2O_2 concentrations (50 mM and 100 mM), moving stomatocytes exhibited indeed a nonlinear fitting, at relatively large Δt (0.51 s). By correlating fuel concentration to the MSD curve fitting (and its slope) it was observed the lower the fuel concentration the slower the nanomotors move, leading to a transition from an MSD parabolic fit to a linear fit, suggesting a

change of the propulsion mechanism from propulsive to diffusive. At high fuel concentrations, bubble propulsion is expected to contribute to motion, which is expect to diminish any effect of rapid τ_r. Therefore, we used the MSD curves (and velocities which were extracted from the fitting of the average MSDs) as a qualitative indication on how active our motors are as a result of their transient binding or unbinding to ATP.

The movement of the nanoparticles was recorded using NTA. The trajectories of the particles were analyzed using NTA software, which registers the corresponding X and Y coordinates. The NTA software tracks the displacement of each particle on a frame-by-frame basis. The recorded trajectories allow for accurate determination of the Brownian particle displacement or mean square displacement (MSD) of every particle, using equations (1) – (3):

$$MSD = \langle \Delta r^2(t) \rangle = \langle \frac{1}{N} \sum_{i=0}^{N} (r_i(t) - r_i(0))^2 \rangle \quad (1)$$

where r = radius and t = sampling time

$$MSD(t) = 2dD \quad (2)$$

where D is the diffusion coefficient and d = dimensionality (in our case for the NTA measurements, d=2),

$$\frac{\overline{(x,y)^2}}{4} = D = \frac{TK_\beta}{3\pi\eta d_H} \quad (3)$$

which is the Stokes Einstein equation where K_B = Boltzmann constant, η = sample viscosity, T = temperature (K), and d_H = hydrodynamic diameter. The NTA 2.2 software from Nanosight automatically detected a total number of 1865 particles in 942 frames. Of this sample 20 particles were tracked – providing statistically enough number of tracks in order to determine the speed.

A typical reaction mixture for movement analysis was based on 10 µL of a mixture of stomatocytes filled with platinum nanoparticles. The obtained solution (10 mg mL^{-1} polymer concentration) was diluted at least 500 times with MES buffer (5 mM), attaining a concentration of particles between 10^7 mL^{-1} and 10^9 mL^{-1}, measured by NTA. Subsequently, 100 mM fuel was added and the stomatocyte nanomotors were injected into the Nanosight chamber for measurement of their movement.

In a typical procedure, PtNP encapsulated stomatocytes were diluted to the appropriate concentration of 1-9 × 10^8-10^9 particles per milliliter, then 10 µL H_2O_2 (35% vol/vol) was added to 1 mL PtNP encapsulated PLL-stomatocytes. The mixture was immediately injected into the sample cell of the Nanosight. A typical video of 30 seconds was recorded. By averaging over

20 nanoparticles within the major size distribution from Nanosight, we obtained the MSD, which was plotted versus the time intervals. (Please note that particles that show drift (due to gas production for example) have been excluded from the MSD calculation. This is an automated process, in which the NTA software cannot track such particles for sufficient time periods and therefore, it clearly indicates that such trajectories are *FALSE*, and therefore cannot be used.) Only *TRUE* trajectories have been used for the MSD analysis.

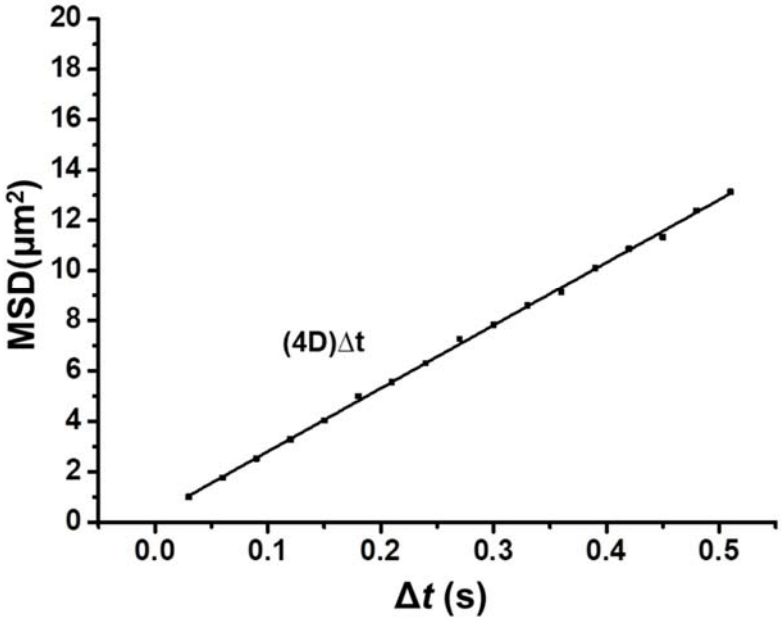

Figure S14. MSD of Pt loaded stomatocytes in the absence of H_2O_2. Please note: these stomatocyte particles exhibited typical Brownian motion and therefore, the equation (4D)Δt was used for fitting.

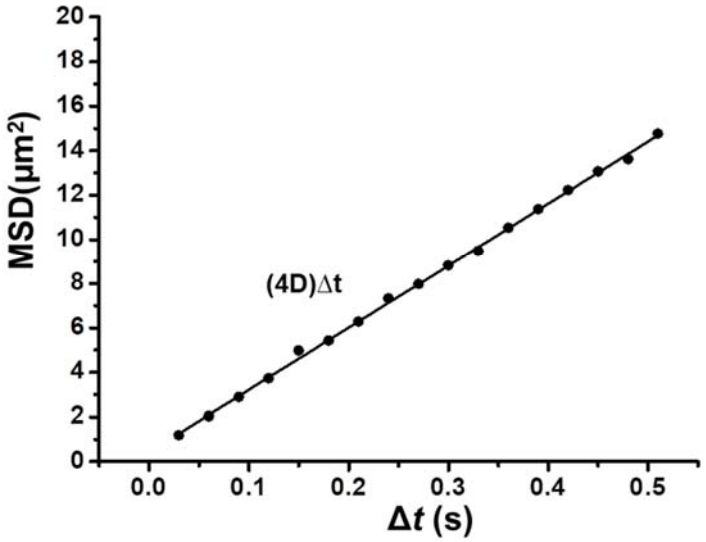

Figure S15. MSD of empty stomatocytes in the presence of 50 mM H_2O_2. Please note: these stomatocyte particles exhibited typical Brownian motion and therefore, the equation (4D)Δt was used for fitting.

ATP-mediated movement analysis

To 10 mL PtNP encapsulated PLL-stomatocytes with a concentration of 1-9 × 10^8-10^9 particles per milliliter was added 10 μL ATP to close the opening of the stomatocytes. Then 100 μL H_2O_2 (35% vol/vol) was added to the ATP-containing nanomotor solution, and10 mL of the sample was immediately taken out to do an NTA measurement. At every time point, particles were tracked for 60 s. The MSD and velocity of the motors were calculated from 20 nanoparticles. To study the influence of ATP on the movement of the motors, ATP was added at four different final concentrations 0 μM,12.5 μM, 25 μM, 37.5 μM, 50 μM and 62.5 μM.

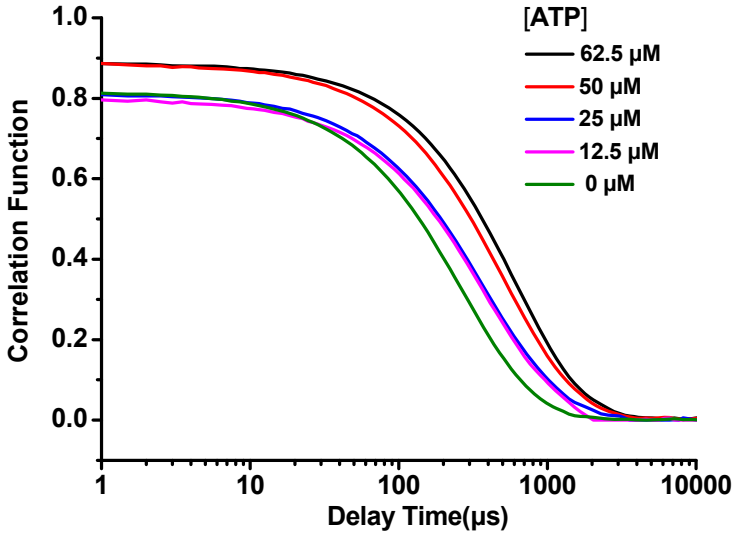

Figure S16. DLS correlation data showing the apparent increase in hydrodynamic size of the PLL-stomatocyte nanomotors with the increase of ATP concentrations in the presence of 100 mM H_2O_2.

Table S3 DLS results of PLL-stomatocyte nanomotors in presence of different concentrations of ATP.

ATP concentration (μM)	Size (nm)
0	298
12.5	317
25	378
50	388
62.5	408

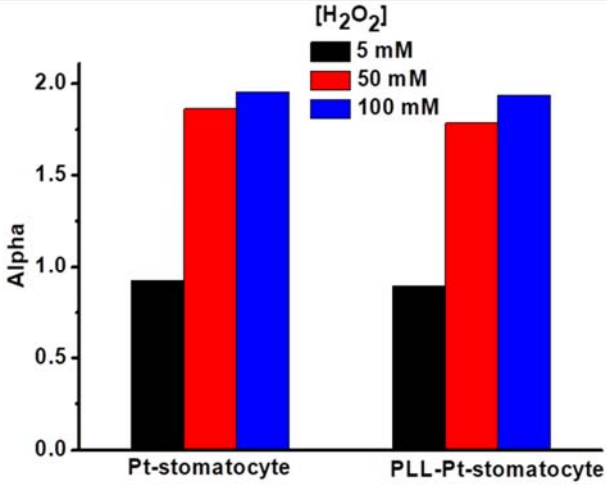

Figure S17. Alpha values of Pt-stomatocytes and PLL-Pt-stomatocytes in presence of 5 mM, 50 mM and 100 mM H_2O_2, respectively.

Table S4 The effect of ATP concentrations on the values of alpha and D_t.

[ATP] (μM)	62.5	50	37.5	25	12.5	0
Alpha	1.16	1.31	1.47	1.70	1.82	1.91
D_t ($\mu m^2/s$)	1.42	1.77	2.39	5.12	5.12	5.12

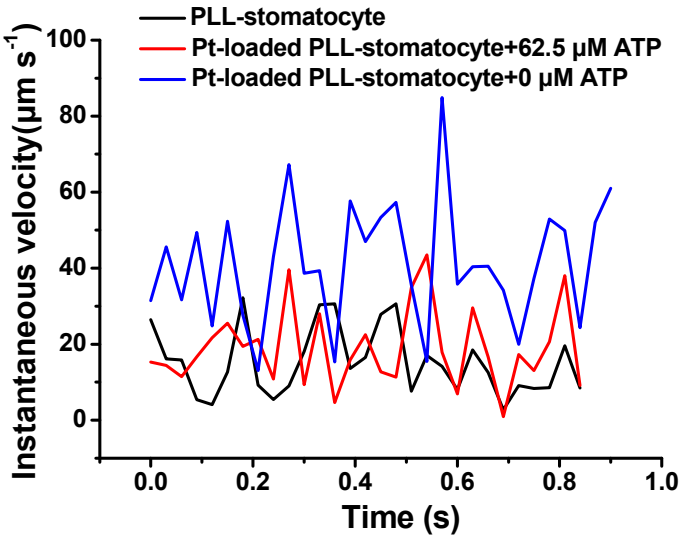

Figure S18. Instantaneous velocity of the nanomotors in the presence of 62.5 and 0 μM ATP with 50 mM H_2O_2 as fuel. Empty PLL-stomatocyte was used as a control.

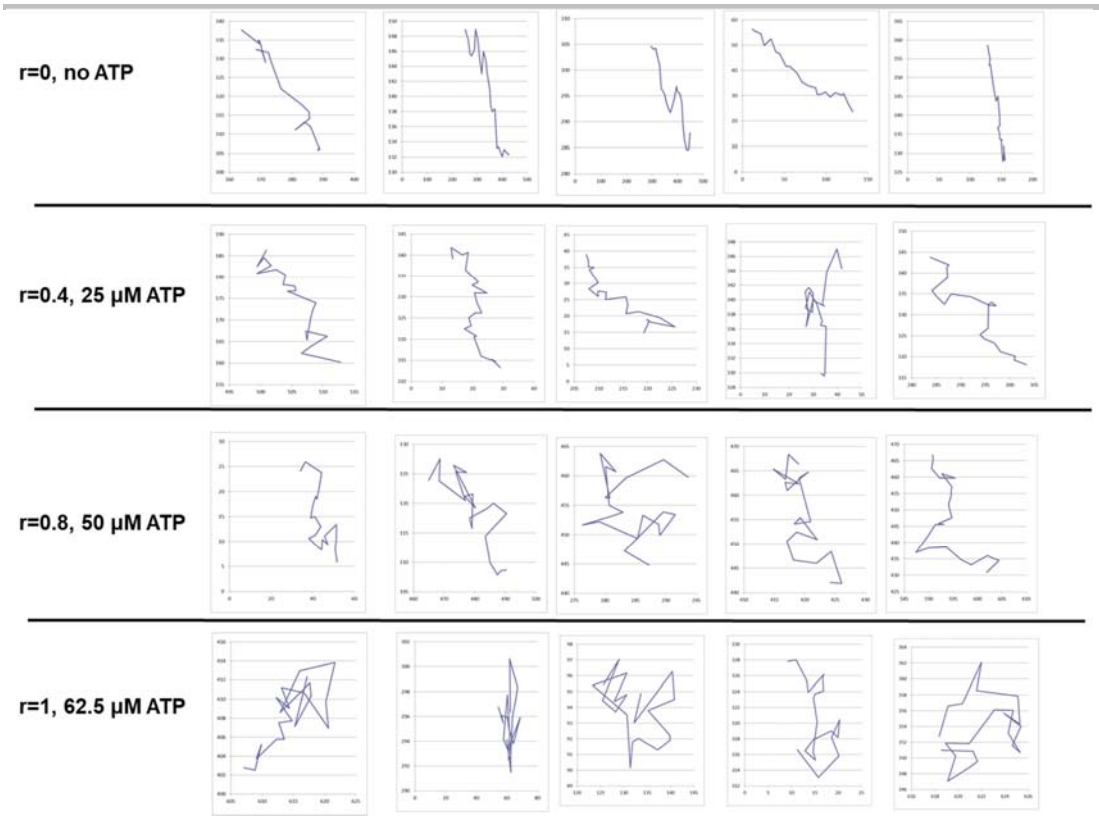

Figure S19. The trajectories of Pt loaded PLL-stomatocyte nanomotors in the presence of different ATP levels.

In a control experiment, AMP (125 μM) was applied instead of ATP (62.5 μM). It was found that the MSD and velocity of the motors did not show any difference in the presence or absence of AMP (Figure S20).

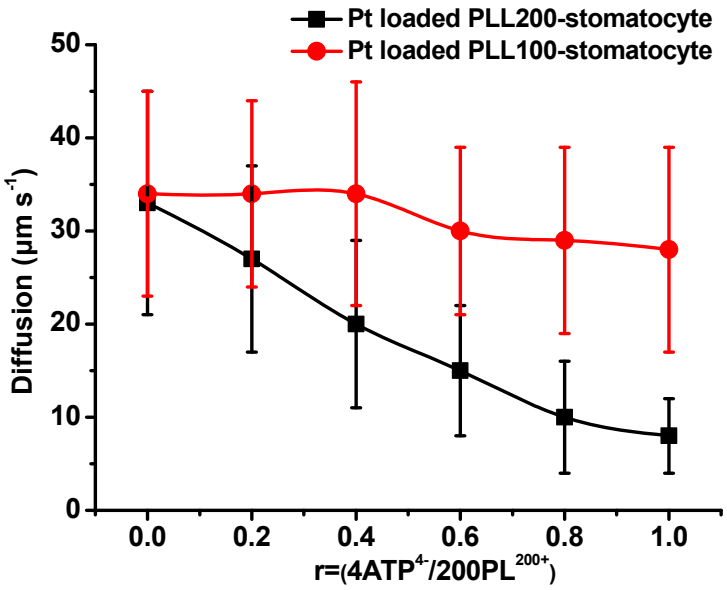

Figure S20. Velocity of PtNP loaded PLL200-stomatocytes and PLL100-stomatocytes (control) in the presence of ATP at different concentrations. Error bars show the s.d. of the velocity of 20 particles.

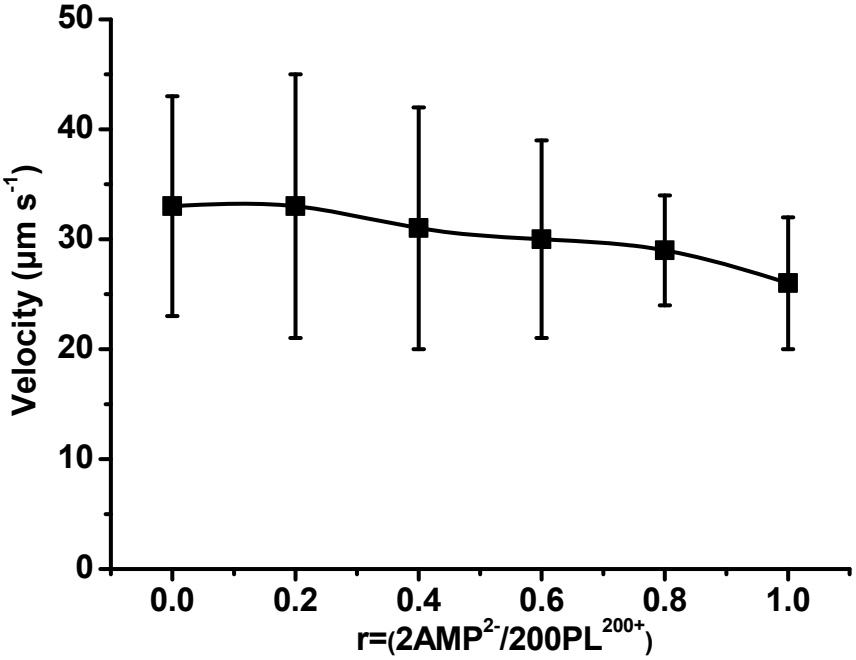

Figure S21. Velocity of the PLL-stomatocyte nanomotors in the presence of AMP at different concentrations. Error bars are based on the measurement of 20 nanomotors.

To demonstrate the adaptive motion of the system, 10 µL apyrase was first introduced in a 10 mL motor solution, then 100 µL H_2O_2 (35% vol/vol) was added. The sample was immediately taken out to do an NTA measurement, after which ATP(r=1) was added. The MSD and velocity of the system before and after addition of ATP were determined, respectively. When the velocity of the nanomotors remained constant, fresh ATP was added again to activate the second cycle. The effect of apyrase concentration (0.1 U mL^{-1} and 0.15 U mL^{-1}) on the adaptive behavior was investigated in the presence of ATP at a constant concentration (62.5 µM).

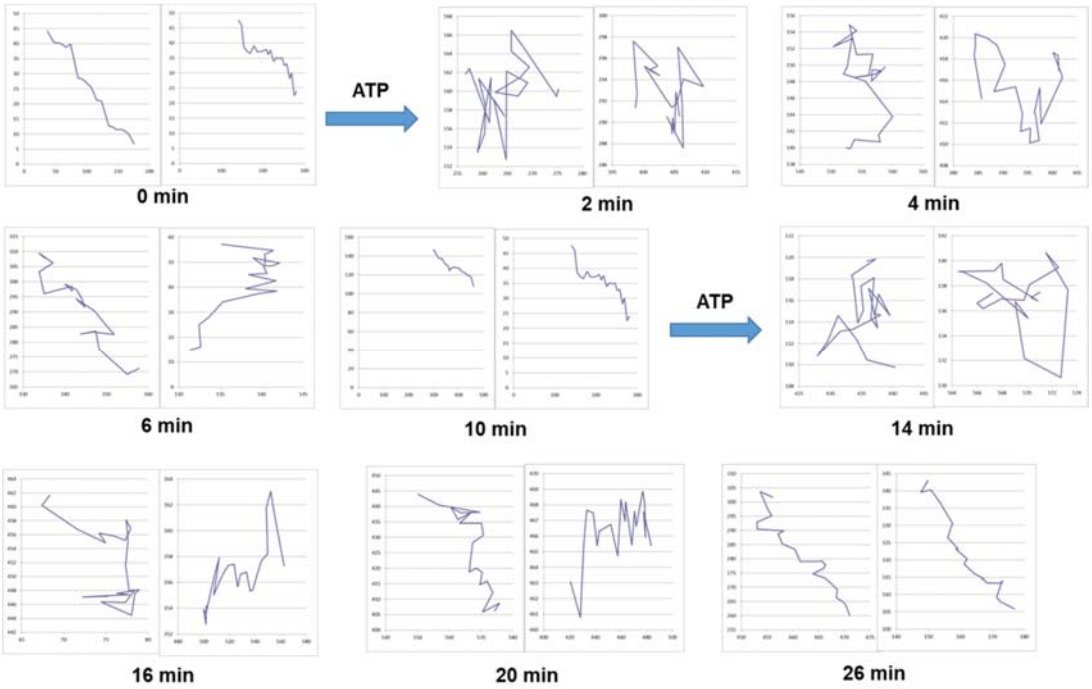

Figure S22. The trajectories of PtNP loaded PLL-stomatocyte nanomotors upon the repeated addition of ATP (62.5 µM). Two automatic on-off cycles of the movement were recorded.

To study the durability of the motors, the movement analysis was conducted over a period of 40 min, the velocity of the particles was calculated according to MSDs fitting. The speed of the motor remained constant, showing that sufficient H_2O_2 supported the sustained production of O_2 (Figure S23).

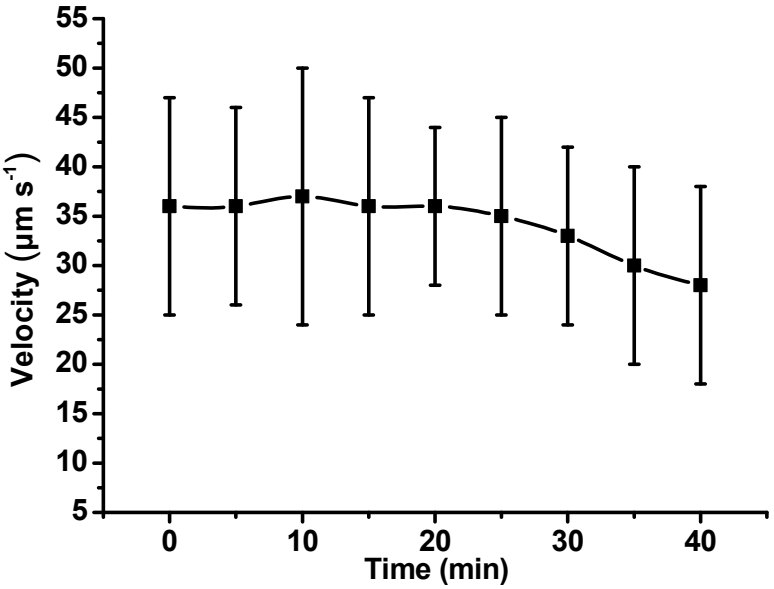

Figure S23. Velocity of the PtNPs loaded PLL-stomatocytes as a function of time in the absence of ATP (100 mM H_2O_2).

References

[1] R. Mahou, C. Wandrey, *Polymers* **2012**, *4*, 561-589.
[2] H. Che, S. Cao, J. C. M. van Hest, *J. Am. Chem. Soc.* **2018**, *140*, 5356-5359.
[3] E. Kim, J. Yang, H.-O. Kim, Y. An, E.-K. Lim, G. Lee, T. Kwon, J.-H. Cheong, J.-S. Suh, Y.-M. Huh, *Biomaterials* **2013**, *34*, 4327-4338.
[4] a) D. A. Wilson, R. J. Nolte, J. C. M. van Hest, *Nat. Chem.* **2012**, *4*, 268; b) M. Nijemeisland, L. K. Abdelmohsen, W. T. Huck, D. A. Wilson, J. C. M. van Hest, *ACS Cent. Sci.* **2016**, *2*, 843-849; c) L. K. Abdelmohsen, M. Nijemeisland, G. M. Pawar, G.-J. A. Janssen, R. J. Nolte, J. C. M. van Hest, D. A. Wilson, *ACS Nano* **2016**, *10*, 2652-2660.
[5] J. R. Howse, R. A. Jones, A. J. Ryan, T. Gough, R. Vafabakhsh, R. Golestanian, *Phys. Rev. Lett.* **2007**, *99*, 048102.